[26]The scaling functions are even in our derivation because they are essentially the scaling functions for the ordinary lattice gas, which are even as a consequence of particle-hole symmetry. Once (3.2) is adopted generally, however, there seems no reason not to relax this constraint, retaining it only to low-enough order to account for such properties as the continuity of the pressure, the symmetry of $\rho_L - \rho_c$ and $\rho_c - \rho_V$, the equality of the density fluctuations in the liquid and vapor phases to leading order, and the fact that $\ddot{\mu}(\rho_c, T)$ does not appear to diverge as strongly as $t^{-(\alpha+\beta)}$. If the evenness assumption is dropped, however, the conjugate-state property no long holds, and the equation is then more general than that of Widom and Stillinger in which the conjugate-state property is inherent.

[27]In some of the models of M. E. Fisher and B. U. Felderhof [Ann. Phys. (N.Y.) 58, 176 (1970)], $\ddot{P}$ and $\ddot{\mu}$ have the same singularity which exceeds that of the heat capacity. However, these models are so peculiar (for example, the coexistence curve is not symmetric even to leading order, so that $\dot{\rho}_d \sim t^{\beta-1}$) that they fall outside even the proposal of Sec. V.

[28]The divergence in $\ddot{\mu}$ cannot be more rapid than $t^{-(\alpha+\beta)}$ (see Ref. 18, note 6) and therefore $n=2$ is the only case likely to produce serious trouble.

[29]Note that this problem cannot be circumvented by making ζ an analytic function of T and $\mu - \mu(T)$, where $\mu(T)$ is the singular phase boundary, for this would introduce spurious singularities into the pressure away from the critical point, at $\tau = 0$ for nonzero ζ.

[30]This is not in contradiction to our remark in Ref. 21. There can be more than one preferred direction, as long as none of them are the P, μ, or T axes. It is, however, weaker than the form stated by Griffiths and Wheeler, who postulate a *single* preferred direction, not parallel to the axes.

[31]See Refs. 13 and 20.

PHYSICAL REVIEW A VOLUME 8, NUMBER 1 JULY 1973

Transition Probabilities of Xe I and Xe II†

Myron H. Miller and Randy A. Roig*
Institute for Fluid Dynamics and Applied Mathematics, University of Maryland, College Park, Maryland 20742

Roger D. Bengtson
Department of Physics, University of Texas at Austin, Austin, Texas 78712

(Received 26 December 1972)

Absolute transition probabilities of the stronger Xe I and Xe II lines between 3800 and 8400 Å are measured in emission. State variables of the shock-tube plasmas are determined by several independent methods. Accuracies for 25 neutral and 128 ionic A values are estimated to be (22–50)%. Experimental Xe I line strengths are compared with theoretical predictions. The Xe II results are examined for conformity with quantum-mechanical sum rules and are compared with lifetime data from the literature.

I. INTRODUCTION

Neutral and ionic line strengths of the lighter rare gases have been intensively investigated, but to date no experimental A values have been available for the leading visible arrays of Xe I or Xe II.[1] Intermediate coupling and configuration mixing are felt to interfere with the application of existing theoretical Xe I line strengths[2] and measured Xe II radiative lifetimes[3,4] towards the development of xenon lasers.[5] This investigation measures A values of the brightest isolated visible lines of the first two xenon spectra, on a sufficiently comprehensive scale that ionic results can be tested against quantum-mechanical sum rules.

II. EXPERIMENTAL

A conventional gas-driven shock tube provided the plasmas. The luminous gas behind first – or multiply – reflected shock waves was quiescent and essentially homogeneous for spectroscopic test times of 30–90 μsec. Test gases were composed of neon containing small concentrations of xenon and either silane (SiH_4) or argon plus krypton. The Balmer profiles resulting from the addition of silane were useful for determining the temperature and electron density of the light source and provided internal radiation standards for the measurement of xenon transition probabilities. The increased Stark-effect broadening occurring when Ar and Kr were plasma constituents minimized radiative trapping in the centers of the brightest Xe II profiles.

Table I is a compendium of the source conditions used in these investigations. The shock tube was operated over the widest temperature-density range compatible with useful signal-to-noise ratios. This was done to selectively enhance the first or second spectrum and to test measured absolute A values for possible dependence upon source conditions.

The following description of the apparatus is less detailed than the accounts given in earlier papers.[6] Multichannel photoelectric recording

TABLE I. Experimental conditions used to determine xenon transition probabilities.

Gases added to neon carrier	Temperature range (10^3 °K)	Pressure range (10^6 dyn/cm^2)	Experimental runs
1.92% Ar + 1.05% Kr + 0.63% Xe	10.2–12.4	6.3–22.0	18
0.27% SiH_4 + 1.09% Xe	10.4–12.5	7.6–28.7	25

was employed for determinations of plasma state and to transfer absolute intensity calibrations[7,8] to a pair of time-resolved spectrograms. In each experiment, xenon spectra were recorded simultaneously[9] on two emulsions having distinctly different response characteristics (γ curves) and spectral sensitivities, using instruments with first-order resolutions 0.24 and 2.3 Å and effective wavelength coverages of 1700 and 6000 Å, respectively. For each emulsion, γ and spectral-response curves were established by two or more independent calibrations.[6] The computer codes which converted digitized spectral densities into relative intensities used temperature and absolute intensity data to reconstruct line profiles in the optically thin limit.[10]

Relative integrated intensities of bright ionic line pairs simultaneously recorded by the two spectrographs agreed in a typical experiment within the jitter due to grain noise and reading error (10–20%): No trends could be associated with the use of different emulsion types or instrumental profiles. The histogram in Fig. 1 shows the measured ratio of strengths for two prominent isolated ionic lines, Xe II λ4213/Xe II λ4603. If the random error is normally distributed, as is indicated by the figure, then error in the mean due to scatter is less than 3%. Faintness and susceptibility to blending by Stark-effect broadening appreciably increase the jitter in typical Xe I results over that illustrated here.

Four temperature measurements[6] were obtained for each of the 25 experiments having silane as a test-gas constituent. The absolute integrated intensities of Ne I(λ5852 Å) and H_β, and pressure data, were inverted to yield excitation temperatures for energy levels 17 and 12 times greater, respectively, than mean thermal energies. The blackbody intensity at λ6562 Å was found by using a pulsed-flash lamp to perform a line-reversal measurement.[8] Application of the Planck relation, in turn, yielded the plasma's radiation temperature. Electron densities obtained by fitting experimental H_β profiles to theoretical Stark shapes[11] were combined[12] with pressure data to determine ionization temperatures in the light source. No systematic differences could be detected between these temperatures. Estimated accuracy of their mean for a typical run was 2–3%. Since the Balmer lines were not present in the 18 experiments using Xe + Kr + Ar additives, only the neon excitation and the blackbody temperatures were available. In these runs, the adopted temperatures had a typical estimated reliability of 3–5%.

The absolute A value of a neutral or ionic line was determined from its integrated emitted intensity $I_{\mathrm{XeI,II}}$ via

$$A^{\mathrm{emis}}_{\mathrm{XeI,II}} = \frac{4\pi\lambda}{hcl}\frac{I_{\mathrm{XeI,II}}}{N_{\mathrm{XeI,II}}}, \tag{1}$$

where N_{XeI} (N_{XeII}) is the excited-state density of a neutral (ionic) xenon line and l is the source thickness in the line of sight.

In a multicomponent plasma, one can obtain another determination of the transition probability by measuring the intensity ratio $I_{\mathrm{XeI,II}}/I_{\mathrm{ref}}$, where I_{ref} is the integrated intensity of some emission line whose A value is comparatively well known. That is,

$$A^{\mathrm{rel\,ref}}_{\mathrm{XeI,II}} = \frac{N_{\mathrm{ref}}}{N_{\mathrm{XeI,II}}}\left(\frac{I_{\mathrm{XeI,II}}}{I_{\mathrm{ref}}}\right)\frac{\lambda_{\mathrm{XeI,II}}}{\lambda_{\mathrm{ref}}}A_{\mathrm{ref}}. \tag{2}$$

These investigations utilized H_β and H_γ (denoted by β and γ, respectively) as internal references

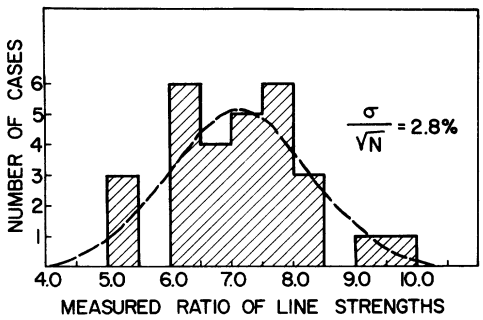

FIG. 1. Histogram of the measured line-strength ratio $S\lambda4213/S\lambda4603$. The dashed curve is a fitted normal-error curve having the same area and σ as the experimental distribution. Uncertainty in the average, 7.13, due to jitter is less than 3%.

TABLE II. Comparison of absolute A-value data.

Transition	Intensity standard	Method	Determinations (n)	A (10^8 sec^{-1})	$\delta/\sqrt{n}$ (%)	Adopted A (10^8 sec^{-1})
Xe II 4603	H_γ	$A^{\text{rel}\,\gamma}_{\text{Xe II}}$	40	0.696	4	0.69 ± 22%
	carbon arc	$A^{\text{emis}}_{\text{Xe II}}$	10	0.650	10	
Xe I 4671	H_β	$A^{\text{rel}\,\beta}_{\text{Xe I}}$	39	0.008 14	6	0.0081 ± 30%
	carbon arc	$A^{\text{emis}}_{\text{Xe I}}$	9	0.008 06	6	
	Xe II 4603	$A^{\text{rel II}}_{\text{Xe I}}$	36	0.008 23	23	

for Xe I and Xe II determinations. Moreover, because the ionic results could be tested against quantum-mechanical sum rules, these were sometimes used as references for the Xe I A values (in which cases the ionic reference line is denoted by II). These trans-species (or transionization-stage) measurements carry essentially no implicit dependence on the absolute photometric calibrations. Undetected absorption or decomposition of silane prior to firing the shock tube is a possible source of bias for determinations relying on Balmer lines for reference A values. If silane losses systematically exceeded 10%, however, they would have been detectable by (i) significant trends between the temperatures simultaneously measured by four different techniques, and (ii) trends between the $A^{\text{emis}}_{\text{XeI,II}}$ and $A^{\text{rel}\,\beta}_{\text{XeI,II}}$ or $A^{\text{rel}\,\gamma}_{\text{XeI,II}}$ data.

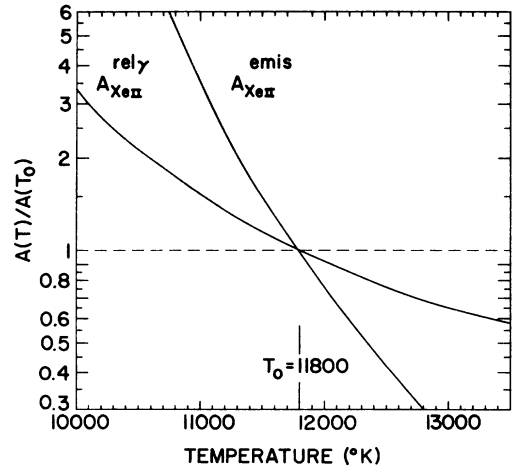

FIG. 2. Sensitivity of experimental Xe II λ4603 transition probabilities to hypothetical errors in temperature data. Measurements in absolute emission $A^{\text{emis}}_{\text{Xe II}}$ and relative to H_γ, $A^{\text{rel}\,\gamma}_{\text{Xe II}}$, incur relative errors $A(T)/A(T_0)$ when the assumed temperature T varies from the true temperature T_0. The analysis applies at a pressure 13.8×10^6 dyn/cm^2 and a test gas composed of 0.27% SiH_4 +1.09% Xe mole concentration in neon.

The temperature dependence implicit in the Xe II transition probabilities measured in absolute emission and by trans-species relative methods is given in Fig. 2. The determinations relative to H_γ are seen to be markedly less sensitive to faulty temperature data than are the A values obtained in absolute emission.

The analogous thermal error analysis for Xe I is given in Fig. 3. For neutral lines, the conventional emission measurements via Eq. (1) have the lesser sensitivity to hypothetical temperature errors T-T_0.

III. RESULTS AND DISCUSSION

The absolute A values of Xe II λ4603 and Xe I λ4671 obtained by the aforementioned redundant experimental techniques are intercompared in Table II. For both the neutral and ionic transitions the independent determinations are in satisfactory agreement, a self-consistency that is reassuring with respect to the possibility of

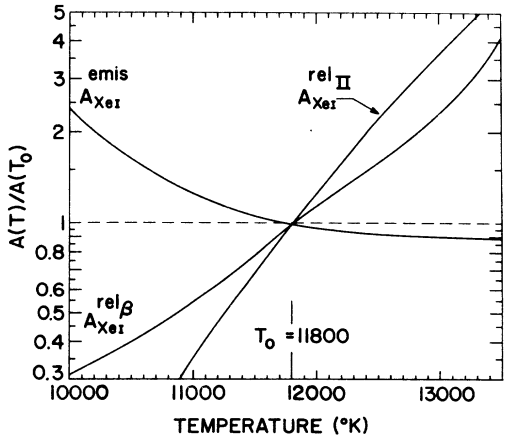

FIG. 3. Implicit thermal dependence of the Xe I λ4671 transition probability measured three ways: in absolute emission $A^{\text{emis}}_{\text{Xe I}}$, relative to H_β, $A^{\text{rel}\,\beta}_{\text{Xe I}}$, and relative to Xe II λ4603, $A^{\text{rel II}}_{\text{Xe I}}$. Plasma pressure and composition are 13.8×10^6 dyn/cm^2 and SiH_4 + 1.09% Xe in neon, respectively.

TABLE III. Transition probabilities for Xe II.

λ_{air} (Å)	Classification (Ref. 13)	g_i-g_k	A values (10^8 sec^{-1}) [a]		λ_{air} (Å)	Classification (Ref. 13)	g_i-g_k	A values (10^8 sec^{-1}) [a]	
3869.6	$5d\ ^4P-6p'\ ^2P^\circ$	2-2	0.25	E	4251.6	$6p\ ^2P^\circ-6d'\ ^2D$	2-4	1.33	B
3954.7	$5d'\ ^2F-15^\circ$	6-6	0.20	C	4269.8	$6s\ ^4P-6p\ ^2P^\circ$	2-2	0.10	C
3972.6	$6p'\ ^2F^\circ-6d'\ ^2F$	6-6	0.84	D	4296.4	$6p\ ^4P^\circ-7s\ ^4P$	4-2	0.72	A
3990.3	$6p\ ^4P^\circ-20$	2-2	0.40	E	4310.5	$6p\ ^2D^\circ-7s'\ ^2D$	6-6	0.49	B
4002.4	$5d''\ ^2D-35^\circ$	4-6	0.42	E	4321.8	$6s\ ^4P-6p\ ^2D^\circ$	2-4	0.05	C
4025.2	$5d\ ^2D-6p'\ ^2P^\circ$	4-2	0.07 [b]	D	4330.5	$6p\ ^4D^\circ-6d\ ^4F$	6-8	1.29	A
4037.3	$6p\ ^4P^\circ-18$	4-2	0.49 [c]	C	4335.8	$6p\ ^4D^\circ-8$	6-6	0.02	B
4037.6	$6p\ ^2S^\circ-6d\ ^2D$	2-4			4369.2	$6p\ ^4P^\circ-18$	2-2	1.01	A
4051.3	$6p\ ^4S^\circ-7s'\ ^2D$	4-6	0.10	C	4373.8	$6p\ ^4D^\circ-6d\ ^4F$	4-4	0.32	B
4057.5	$6p\ ^4P^\circ-6d\ ^4F$	6-8	0.22	B	4393.2	$6p\ ^4S^\circ-6d\ ^2D$	4-6	1.58	A
4098.9	$6p\ ^4P^\circ-12$	2-4	0.29	D	4395.8	$5d'\ ^2F-4f'\ ^2F$	6-8	0.52	A
4100.3	$5d\ ^4D-6p\ ^4D^\circ$	4-2	0.05 [d]	D	4406.9	$6p\ ^2P^\circ-6d\ ^2D$	4-4	0.62	B
4105.0	$5d\ ^2P-6p'\ ^2P^\circ$	4-4	0.64	D	4414.8	$5d\ ^2D-6p'\ ^2D^\circ$	6-6	0.42	A
4110.4	$5d\ ^4D-6p\ ^2S^\circ$	2-2	0.05	E	4416.1	$6p\ ^2D^\circ-14$	4-6	0.40	B
4158.0	$6p\ ^2S^\circ-6d\ ^2P$	2-2	0.27	C	4441.0	$6p\ ^4S^\circ-6d\ ^4P$	4-4	0.47	E
4162.2	$5d\ ^2D-6p'\ ^2D^\circ$	4-4	0.10	B	4470.9	$5d\ ^2D-6p'\ ^2D^\circ$	6-4	0.10	C
4180.1	$6p\ ^4P^\circ-6d\ ^4D$	4-4	0.42	A	4480.9	$6p\ ^4D^\circ-6d\ ^4F$	4-6	1.33	A
4208.5	$6p\ ^4P^\circ-6d\ ^4D$	4-6	0.54	B	4485.7	$5d\ ^4P-6p'\ ^2P^\circ$	4-4	0.07	D
4209.5	$6p\ ^4P^\circ-6d\ ^4D$	6-4			4532.5	$6s'\ ^2D-6p'\ ^2F^\circ$	6-8	0.21	A
4213.7	$6p\ ^4D^\circ-6d\ ^4P$	2-4	1.2	E	4536.9	$6p\ ^4P^\circ-6d\ ^4D$	2-4	0.21	A
4215.6	$6s\ ^4P-6p\ ^4D^\circ$	6-4	0.15	E	4540.9	$6p\ ^2D^\circ-7s'\ ^2D$	4-6	1.41	A
4223.0	$6p\ ^2P^\circ-14$	4-6	1.48	B	4545.2	$6p\ ^4D^\circ-6d\ ^4D$	6-8	0.42	A
4238.3	$6p\ ^4P^\circ-6d\ ^4D$	6-6	0.91	A	4555.9	$6p\ ^4D^\circ-20$	4-2	0.57	E
4245.4	$6p\ ^4P^\circ-6d\ ^4D$	6-8	0.74 [e]	B	4577.1	$6p\ ^4D^\circ-6d\ ^4D$	8-6	0.35	B
4585.5	$6p\ ^4D^\circ-6d\ ^4D$	8-8	1.01	A	4887.3	$6s\ ^2P-6p\ ^2P^\circ$	4-4	0.42	A
4592.1	$6p\ ^4S^\circ-6d\ ^4P$	4-6	0.89	B	4890.1	$6s\ ^4P-6p\ ^4D^\circ$	6-6	0.10	B
4603.0	$6s\ ^4P-6p\ ^4D^\circ$	4-4	0.69	A	4919.7	$6s\ ^2P-6p\ ^2P^\circ$	2-2	0.74	B
4615.1	$6p\ ^4P^\circ-4$	4-2, 4	0.30 [f]	E	4921.5	$6s\ ^2P-6p\ ^2D^\circ$	4-6	1.23	A
4615.5	$6s'\ ^2D-6p'\ ^2P^\circ$	6-4	0.47 [f]	E	4972.7	$5d\ ^2D-6p'\ ^2P^\circ$	6-4	0.96 [k]	B
4617.5	$6p\ ^2D^\circ-6d\ ^2D$	4-4	1.11	E	4988.7	$6s\ ^2P-6p\ ^2D^\circ$	2-4	0.35	B
4633.3	$5d\ ^4F-6p\ ^2D^\circ$	6-6	0.06	B	5080.6	$6p\ ^4D^\circ-7s\ ^4P$	6-4	1.70 [l]	B
4651.9	$6s\ ^2P-6p\ ^2D$	4-4	0.35	A	5122.4	$6p\ ^4P^\circ-7s\ ^4P$	2-4	0.05	E
4668.5	$5d''\ ^2D-6p'\ ^2P^\circ$	4-2	0.59	A	5125.7	$6d'\ ^2D-6p'\ ^2D^\circ$	6-6	0.54	E
4672.2	$6p\ ^4P^\circ-7s\ ^4P$	4-4	0.49	B	5178.8	$5d\ ^2D-6p'\ ^2F^\circ$	6-6	0.42	E
4698.0	$6p\ ^4D^\circ-12$	4-4	1.29	B	5184.5	$6s'\ ^2D-6p'\ ^2D^\circ$	4-6	1.23	E
4715.2	$6p\ ^2S^\circ-7s\ ^2P$	2-4	0.57	C	5188.1	$6p\ ^2D^\circ-7s\ ^2P$	6-4	4.9	D
4731.2	$6p\ ^2P^\circ-6d\ ^2D$	4-6	3.7 [g]	C	5191.4	$6s\ ^4P-6p\ ^4D^\circ$	2-2	3.2	A
4769.1	$5d\ ^2D-6p'\ ^2F^\circ$	4-6	0.20	B	5260.4	$6s\ ^2P-6p\ ^2P^\circ$	2-4	1.1 [m]	D
4773.2	$5d''\ ^2D-15^\circ$	6-6	0.25	C	5261.9	$6s'\ ^2D-6p'\ ^2D^\circ$	4-4	5.43	B
4779.2	$5p^6\ ^2S-6p\ ^4P^\circ$	2-4	0.05	C	5292.2	$6s\ ^4P-6p\ ^4P^\circ$	6-6	2.32	A
4787.8	$5d'\ ^2D-6p'\ ^2D^\circ$	4-6	0.22 [h]	C	5309.3	$6s\ ^2P-6p\ ^4S^\circ$	4-4	0.94	B
4818.0	$5d\ ^4D-6p\ ^4D^\circ$	4-4	0.12 [i]	C	5313.9	$6p\ ^4D^\circ-7s\ ^4P$	8-6	3.46	B
4823.4	$6p\ ^4P^\circ-7s\ ^4P$	4-6	0.49	A	5339.4	$6s\ ^4P-6p\ ^4P^\circ$	6-4	1.88 [n]	B
4844.3	$6s\ ^4P-6p\ ^4D^\circ$	6-8	0.77	A	5363.3	$6p\ ^2D^\circ-7s\ ^2P$	4-6	1.21	C
4862.5	$6p\ ^4P^\circ-7s\ ^4P$	6-6	0.72	A	5368.1	$5d\ ^2P-6p\ ^2P^\circ$	2-2	1.29	B
4876.5	$5d\ ^2D-6p'\ ^2F^\circ$	6-8	0.94	A	5372.4	$6s\ ^4P-6p\ ^4P^\circ$	4-2	2.76	B
4883.5	$6s\ ^4P-6p\ ^4S^\circ$	2-4	0.77	B	5419.2	$6s\ ^4P-6p\ ^4D^\circ$	4-6	2.13	B
4884.1	$6p\ ^4D^\circ-6d\ ^4P$	2-2	1.58 [j]	E	5439.0	$6s\ ^2P-6p\ ^2S^\circ$	4-2	3.76	B
5450.5	$5d\ ^2P-6p\ ^2D^\circ$	2-4	0.37 [p]	D	5976.5	$6s\ ^4P-6p\ ^4P^\circ$	4-4	1.09	D
5460.4	$5d\ ^4D-6p\ ^4D^\circ$	6-8	0.27	B	6036.2	$5d\ ^4D-6p\ ^4P^\circ$	6-6	0.15	C
5472.6	$5d\ ^4D-6p\ ^4D^\circ$	8-8	0.49	B	6051.2	$5d\ ^4D-6p\ ^4P^\circ$	8-6	0.52	D
5531.1	$5d\ ^4D-6p\ ^4D^\circ$	8-6	0.12	C	6097.6	$5d\ ^4D-6p\ ^4P^\circ$	6-4	0.72	B
5616.7	$5d\ ^2P-6p\ ^2D^\circ$	4-6	0.35	C	6101.4	$5d\ ^2D-6p\ ^2D^\circ$	4-4	1.46	E
5659.4	$5d\ ^2P-6p\ ^2P^\circ$	2-2	1.30	D	6270.8	$6s'\ ^2D-6p'\ ^2F^\circ$	4-6	0.89	E
5667.6	$5d\ ^4D-6p\ ^4P^\circ$	4-2	1.23	C	6277.5	$5d\ ^4D-6p\ ^4P^\circ$	4-6	0.15	E
5699.6	$5d'\ ^2D-6p'\ ^2F^\circ$	4-6	0.74	C	6300.9	$5d\ ^2P-6p\ ^2S^\circ$	4-2	0.62	E
5716.2	$6p'\ ^2D^\circ-6d'\ ^2D$	6-6	18.5	E	6344.0	$5d\ ^4D-6p\ ^4P^\circ$	4-4	0.82	E
5726.9	$6p\ ^4P^\circ-5d''\ ^2S$	4-2	0.08 [g]	E	6356.4	$5d''\ ^2D-15^\circ$	4-6	27.00	D
	$5d'\ ^2F-6p'\ ^2D^\circ$	6-6			6375.3	$5d\ ^2P-6p\ ^4S^\circ$	2-4	0.62	E

TABLE III *(Continued)*

λ_{air} (Å)	Classification (Ref. 13)	g_i-g_k	A values (10^8 sec^{-1})[a]	λ_{air} (Å)	Classification (Ref. 13)	g_i-g_k	A values (10^8 sec^{-1})[a]
5751.0	$5d\ ^2P - 6p\ ^2D^\circ$	2-4	1.06 *C*	6512.8	$5d\ ^2D - 6p\ ^2P^\circ$	4-4	0.49 *E*
5758.7	$5d'\ ^2D - 6p'\ ^4F^\circ$	6-8	0.94 *C*	6528.7	$5d'\ ^2F - 6p'\ ^2F^\circ$	6-8	0.42 *E*
5776.4	$5d\ ^2P - 6p\ ^2P^\circ$	2-4	0.61 *D*	6694.3	$5d\ ^4D - 6p\ ^4P^\circ$	2-4	0.62 *D*
5843.3	$5d'\ ^2D - 6p'\ ^2P^\circ$	6-4	1.16[r] *E*	6910.2	$5d\ ^2P - 6p\ ^4D^\circ$	2-2	0.20 *E*
5905.1	$6s\ ^2P - 6p\ ^2S^\circ$	2-2	0.79 *E*	6990.9	$5d\ ^4F - 6p\ ^4D^\circ$	4-8	0.27 *C*
5971.1	$6s'\ ^2D - 6p'\ ^2P^\circ$	4-4	1.30 *E*	7164.8	$5d'\ ^2F - 6p'\ ^2F^\circ$	8-6	0.69 *E*

[a] Uncertainty: $22\% \le A \le 25\%$; $25\% < B \le 30\%$; $30\% < C \le 40\%$; $40\% < D \le 50\%$; $50\% < E$.
[b] Blending with 4026.2 is troublesome.
[c] Blend has two lines of comparable brightness with difference in upper level energy of 1 eV. Mean upper-level energy used to compute A is $\Sigma(gA)/g$.
[d] Blending with 4100.97 is troublesome.
[e] Some blending with 4244.4.
[f] Complete blending: data of Striganov and Sventitskii (Ref. 13) used for intensity resolution.
[g] Blend with 4732.5 [$I \approx \frac{1}{6} I(4731.2)$].
[h] Some blending with 4786.6.
[i] Blended with 4817.2: Striganov and Sventitskii (Ref. 13) indicate $I4817.2 \approx \frac{1}{10} I4818.0$.
[j] Blending in wings with 4883.5.
[k] Blended with 4971.7: Striganov and Sventitskii (Ref. 13) indicate $I4971.7 \approx \frac{1}{10} I4972.7$.
[l] Blend with 5081.1: Striganov and Sventitskii (Ref. 13) indicate $I5081.1 \approx \frac{1}{20} I5080.6$.
[m] Blend with 5259.9: Striganov and Sventitskii (Ref. 13) indicate $I5259.9 \approx \frac{1}{7} I5260.4$.
[n] Contribution of $6p$–$6d$ to blend ignored.
[p] Blend with 5490.9: Striganov and Sventitskii (Ref. 13) indicate $I5490.9 \approx \frac{1}{5} I5450.5$.
[q] $A = \dfrac{g_1 A_1 + g_2 A_2}{g_1 + g_2}$, using mean upper-state energy.
[r] Blending with $6p'$–14 neglected.

biasing by unrecognized absorption of silane.

Experimental Xe II transition probabilities are presented in Table III. Quoted experimental uncertainties are derived from both observed scatter and best estimates of possible systematic errors.

The Coulomb approximation and LS coupling were used to calculate A values for some of the ionic lines in Table III. For the stronger transitions which one expects to be least affected by configuration mixing and intermediate coupling,[14] semiquantitative agreement (±50%) was generally found between these approximations and the shock-tube data; for weaker lines, however, disagree-

TABLE IV. Comparison of experimental lifetimes for Xe II.

Level	Lifetime ($n$sec) This experiment	Allen *et al.*[a]	Fink *et al.*[b]
$6p\ ^4D^\circ_{3/2}$	10 ±5	7±3	19
$6p'\ ^2P^\circ_{3/2}$	1.7±0.8	5±2	
$6p'\ ^2P^\circ_{1/2}$	11 ±5	5±2	
$6p\ ^4P_{5/2}$	2.6±1.3	13±6	22
$6p\ ^4D_{5/2}$	4 ±2	11±5	19

[a] Reference 3. [b] Reference 4.

TABLE V. Transition-array average f values for $6p$ levels in Xe II compared with one-electron sum rules.

Final state	ns	nd
$n=5$	···	−0.66
$n=6$	−0.80	0.60
$n=7$	0.59	0.65[a]
$n=8$	0.02[a]	0.16[a]
$n=9 \to \infty$	0.04[a]	0.20[a]
$n \to$ continuum	0.01[a]	0.11[a]
Partial sum	−0.14	1.06
Sum rule[b]	−0.11	1.11
Total sum	0.92	
Sum rule[c]	1.00	

[a] Hydrogenic approximations (Ref. 16).
[b] Reference 15.
[c] Reference 16.

TABLE VI. Transition probabilities for Xe I.

λ_{air} (Å)	Classification (Ref. 13)	g_i-g_k	A values (10^8 sec^{-1}) this experiment [a]		Chen and Garstang (Ref. 2)
4078.8	$6s\,[1\frac{1}{2}]°-8p\,[\frac{1}{2}]$	3-1	0.49	C	•••
4193.0	$6s\,[1\frac{1}{2}]°-4f\,[2\frac{1}{2}]$	5-5	0.11	E	•••
4193.5	$6s\,[1\frac{1}{2}]°-4f\,[2\frac{1}{2}]$	5-7			•••
4203.7	$6s\,[1\frac{1}{2}]°-4f\,[1\frac{1}{2}]$	5-5	0.021	D	•••
4383.9	$6s\,[1\frac{1}{2}]°-4f\,[1\frac{1}{2}]$	3-5	0.08	E	•••
4385.8	$6s\,[1\frac{1}{2}]°-4f\,[1\frac{1}{2}]$	3-3	0.23	E	•••
4501.0	$6s\,[1\frac{1}{2}]°-6p'[\frac{1}{2}]$	5-3	0.39	C	1.9
4582.7	$6s\,[1\frac{1}{2}]°-6p'[\frac{1}{2}]$	3-1	0.39	C	•••
4611.1	$6s\,[1\frac{1}{2}]°-7p\,[1\frac{1}{2}]$	5-3	0.26	C	0.51
4624.3	$6s\,[1\frac{1}{2}]°-7p\,[1\frac{1}{2}]$	5-5	0.42	C	2.2
4671.2	$6s\,[1\frac{1}{2}]°-7p\,[2\frac{1}{2}]$	5-7	0.61	C	2.9
4734.2	$6s\,[1\frac{1}{2}]°-6p'[1\frac{1}{2}]$	3-5	0.089	C	1.5
4807.0	$6s\,[1\frac{1}{2}]°-7p\,[\frac{1}{2}]$	3-1	1.52	C	2.6
4829.7	$6s\,[1\frac{1}{2}]°-7p\,[1\frac{1}{2}]$	3-3	0.19	C	2.1
4916.5	$6s\,[1\frac{1}{2}]°-6p'[1\frac{1}{2}]$	3-3	0.25	C	0.03
4923.2	$6s\,[1\frac{1}{2}]°-7p\,[2\frac{1}{2}]$	3-5	0.19	C	1.8
5695.8	$6s'\,[\frac{1}{2}]°-6f\,[1\frac{1}{2}]$	3-5	0.16 [b]	E	•••
5696.5	$6s'\,[\frac{1}{2}]°-6f\,[1\frac{1}{2}]$	3-3			
6182.4	$6p'[2\frac{1}{2}]-8d\,[3\frac{1}{2}]°$	5-7	3.38	C	•••
6318.1	$6p\,[2\frac{1}{2}]-8d\,[3\frac{1}{2}]°$	7-9	2.70	C	•••
6882.2	$6p\,[2\frac{1}{2}]-7d\,[3\frac{1}{2}]°$	5-7	6.4	D	•••
7642.0	$5d\,[1\frac{1}{2}]°-5f'[2\frac{1}{2}]$	5-5	4.3	C	•••
7887.4	$6s'\,[\frac{1}{2}]°-6p\,[\frac{1}{2}]$	3-3	10.4 [c]	D	14.0
8231.6	$6s\,[1\frac{1}{2}]°-6p\,[1\frac{1}{2}]$	5-5	3.8	C	23.00
8280.1	$6s\,[1\frac{1}{2}]°-6p\,[\frac{1}{2}]$	3-1	10.0	C	36.00
8346.8	$6s'\,[\frac{1}{2}]°-6p'[1\frac{1}{2}]$	3-5	6.36	C	35.0
8409.2	$6s\,[1\frac{1}{2}]°-6p\,[1\frac{1}{2}]$	5-3	0.83	C	2.1

[a] Uncertainty: $30\% < C \leq 40\%$; $40\% < D \leq 50\%$; $50\% < E$.
[b] Multiplet A value: $A = \Sigma(gA/g)$.
[c] Blends slightly with second-order Al r resonance line.

ments larger than a factor of 5 were common.

Experimental Xe II lifetimes of Allen *et al.*[3] and Fink *et al.*[4] are compared in Table IV with lifetimes derived from present results by neglecting cascading and lines too faint for measurement in the shock tube. It is estimated that these approximations and experimental error cause uncertainty of not more than 50% in the latter lifetimes. Discrepancies between the three sets of experimental lifetimes clearly exceed the compounded confidence limits.

Measured absorption oscillator strengths for transitions involving $6p$ configurations of Xe II are arranged in Table V for comparison with the f-sum rules.[15,16] Experimental data constitute 90% of the $6p$-ns array sums and 60% of the $6p$-nd array sums—the remainder being calculated in the central-field approximation.[16] The partial f sums for transitions to ns and nd levels both conform satisfactorily to the Wigner-Kirkwood[15] expectation values of -0.11 and 1.11, respectively. The agreement within 8% between the total sum and the Thomas-Reiche-Kuhn expectation value (unity for one-electron systems)[16] is felt to directly support the present absolute scale for Xe II transition probabilities.

Shock-tube transition probabilities for Xe I and comparison values from the literature appear in Table VI. Intermediate-coupling calculations by Chen and Garstang[2] predict A values which are on the average more than three times larger than present results. Moreover, superimposed on this difference in absolute scales are serious discrepancies between the measured and predicted relative A values. The experimental relative line strengths depend primarily on relative intensities recorded simultaneously by the same detector. Uncertainties associated with such measurements are an order of magnitude too small to account for the discrepancies. Treatment of configuration mixing may be needed to upgrade the theoretical predictions.

ACKNOWLEDGMENTS

The authors wish to acknowledge the support and encouragement of T. D. Wilkerson and the attentive work of J. Clawson, which facilitated reduction of the data.

†Research supported in part by National Aeronautic and Space Administration Grant Nos. NGR-21-002-007/8 and GP-29255, and the Welch Foundation. Computer time was provided through National Aeronautic and Space Administration Grant No. NsG-398 to the Computer Science Center of the University of Maryland.

*Present address: Physics Department, Harvard University, Cambridge, Mass. 02138.

[1]B. M. Miles and W. L. Wiese, Natl. Bur. Std. Spec. Publ. No. 320 (U.S. GPO, Washington, D.C., 1970). See also M. H. Miller, R. A. Roig, and R. D. Bengtson, J. Opt. Soc. Am. 62, 1027 (1972).

[2]C. J. Chen and R. H. Garstang, J. Quant. Spectrosc. Radiat. Transfer **10**, 1347 (1970). See also M. Aymar, Physica (Utr.) **57**, 178 (1972).

[3]L. Allen, D. G. C. Jones, and D. G. Schofield, J. Opt. Soc. Am. **59**, 841 (1962).

[4]U. Fink, S. Bashkin, and W. S. Bickel, J. Quant. Spectrosc. Radiat. Transfer **10**, 1241 (1970).

[5]W. L. Faust and R. A. McFarlane, J. Appl. Phys. **35**, 2010 (1964). See also W. B. Bridges, Appl. Phys. Lett. **3**, 45 (1963).

[6]M. H. Miller, R. A. Roig, and R. D. Bengtson, Phys. Rev. A **4**, 1709 (1971); R. D. Bengtson, M. H. Miller, D. W. Koopman, and T. D. Wilkerson, Phys. Rev. A **3**, 16 (1971); M. H. Miller and R. D. Bengtson, Phys. Rev. A **1**, 983 (1970); R. D. Bengtson, M. H. Miller, D. W. Koopman, and T. D. Wilkerson, Phys. Fluids **13**, 372 (1970).

[7]A. T. Hattenburg, Appl. Opt. **6**, 95 (1967).

[8]M. H. Miller and R. D. Bengtson, J. Quant. Spectrosc. Radiat. Transfer **9**, 1573 (1969).

[9]S. M. Wood and M. H. Miller, Rev. Sci. Instrum. **41**, 1196 (1970).

[10]R. A. Bell, R. D. Bengtson, D. R. Branch, D. M. Gottlieb, and R. A. Roig, University of Maryland Report No. BN-572, 1968 (unpublished).

[11]P. Kepple and H. R. Griem, Phys. Rev. **173**, 317 (1968).

[12]H. R. Griem, *Plasma Spectroscopy* (McGraw-Hill, New York, 1964).

[13]A. R. Striganov and N. S. Sventitskii, *Tables of Spectral Lines of Neutral and Ionized Atoms* (Plenum, New York, 1968).

[14]J. C. Slater, *Quantum Theory of Atomic Structure* (McGraw-Hill, New York, 1960), Vol. II.

[15]E. Wigner, Phys. Z. **32**, 450 (1931); J. G. Kirkwood, Phys. Z. **33**, 521 (1932).

[16]H. A. Bethe and E. E. Salpeter, *Quantum Mechanics of One- and Two-Electron Atoms* (Springer, Berlin, 1957).

PHYSICAL REVIEW A VOLUME 8, NUMBER 1 JULY 1973

Theory of Surface Excitations in Fermi Systems of Finite Thickness*

Allan Griffin† and Eugene Zaremba‡

Department of Physics, University of Toronto, Toronto, Ontario, Canada, M5S 1A7

(Received 14 August 1972)

We consider a degenerate system of fermions interacting via a Yukawa potential and confined within a slab of thickness L. Using the semiclassical random-phase approximation, we obtain the retarded density response function $\chi_{nn}(\vec{k}, \vec{k}', \omega)$, which exhibits resonances corresponding to surface, as well as surface-bulk, or mixed, collective excitations. The surface and surface-bulk density fluctuations are spatially either of a symmetric or antisymmetric character. Their dispersion relations and collisionless damping are discussed, mainly in the strong-coupling limit. A symmetric surface mode which is phononlike at long wavelengths is found, but the antisymmetric surface mode ceases to exist below a certain value of $\hat{k}_{\|}$, the wave vector parallel to the surface. The mixed modes all possess an energy gap at $\hat{k}_{\|} = 0$. We also evaluate the dynamic structure factor $S(\vec{q}, \omega)$ which describes the inelastic scattering of particles in the Born approximation. Our calculations exhibit how crucially the nature of collisionless surface modes depends on the range of interaction between quasiparticles. We argue that our model calculations should be appropriate to liquid He^3 in situations where the restricted dimension is of order 100 Å or larger.

I. INTRODUCTION

Recently, Griffin and Harris[1] (hereafter referred to as GH) have discussed the nature of surface modes in two model problems: (a) a two-component degenerate plasma of electrons and ions, and (b) a one-component degenerate system of fermions interacting via short-range (Yukawa) potential. The analysis could be referred to as a semiclassical half-space model, since the static density distribution was taken to be a step function and the dynamics was treated in terms of a collisionless Boltzmann equation, which corresponds to the semiclassical random-phase approximation (RPA).

In the present paper, we shall discuss model (b) for the case in which the system is bounded by two plane surfaces. We shall refer to this as the film or slab geometry, as opposed to the half-space geometry studied by GH. Our main goal will be to obtain the density response function and thereby determine the dispersion relation of the collective density fluctuations in such a finite system. Since the dynamics of the particles is treated in the self-consistent-field approximation, the kind of modes we will be discussing are in the so-